

Hydrodynamically driven docking of blocks for 3D fluidic assembly

Michael Kalontarov · Michael T. Tolley ·
Hod Lipson · David Erickson

Received: 18 December 2009 / Accepted: 18 January 2010
© Springer-Verlag 2010

Abstract In this work we develop a method for fluid dynamically driven assembly in three dimensions and demonstrate its applicability to the development of programmable matter. Towards this end, we investigate docking of a single block onto a larger structure using detailed numerical simulations and experiments. Our simulation results show that a block whose degrees of freedom are limited is able to align parallel with the docking site, a necessary condition for successful assembly, whereas an unconfined block could not. Experiments with blocks that were designed with this approach confirmed alignment parallel with the docking site in 97% of trials. To generate alignment in the other two planes, we designed blocks that self-align due to geometric interactions. We also introduced a pulsating flow to increase the probability of aligned assembly. Using this strategy, a 54% successful (fully aligned) assembly rate was achieved.

Keywords Programmable matter · Self-assembly · Microfluidics · Reconfigurable systems

1 Introduction

Programmable matter is concept by which objects or devices are constructed from a set of fundamental building

blocks that can be automatically assembled, disassembled, and reassembled into various functional forms capable of performing different tasks. Traditional manufacturing techniques are well suited to create devices designed for specific, pre-determined uses. When a new capability is desired or required, via these methods it is often easier to construct an entirely new device rather than try to reconfigure the old one. In an ideal programmable matter system the building blocks only need to be manufactured once and reconfiguration could be done automatically in response to changing needs. The development of such a system would have wide application in robotics, defense, and exploration.

The eventual attainment of such a system requires the development of new assembly methods that can reversibly bring together large numbers of building blocks in a highly parallel manner. At the micro- and nanoscales, fluidic self-assembly is an approach by which this could be achieved. Nano-scale structures have been assembled using lithographically directed self-assembly (Liddle et al. 2004). At the microscale, fluid and capillary-driven self-assembly of microscale actuators, electrical, and optical components has been demonstrated (Srinivasan et al. 2001; Avital and Zussman 2006; Morris and Parviz 2006). Directed self-assembly of microparts has been approached by thermally (Sharma 2007) and electrically (Chung et al. 2006) controlling the binding affinities of capillary force interaction sites. These techniques are useful for the assembly of complex Micro-Electro-Mechanical System (MEMS) devices because they allow large numbers of components that are made by different processes to be integrated in a highly parallel manner (Mastrangeli et al. 2009). Other systems have been developed that allow for the programmable assembly of structures. Chung et al. (2008), for example, demonstrated a system which utilizes a microfluidic rail networks to assemble a wide range of micro-structures from

Electronic supplementary material The online version of this article (doi:10.1007/s10404-010-0572-9) contains supplementary material, which is available to authorized users.

M. Kalontarov · M. T. Tolley · H. Lipson · D. Erickson (✉)
Sibley School of Mechanical and Aerospace Engineering,
Cornell University, 240 Upson Hall, Ithaca, NY 14853,
New York
e-mail: de54@cornell.edu

polymer components. However, a new and specific microfluidic rail network needs to be constructed for every assembly task. Tolley et al. (2008) and Krishnan et al. (2008) demonstrated the directed assembly of silicon tiles using fluid flow in a unstructured microfluidic chamber. Though most of these systems allow for some form of directed assembly, there are two limitations when applied to the development of macroscale programmable matter. The first is that the assembly occurs in 2D in a single plane. The second is that because they are of micro- or nanoscale dimensions, an inordinate number of these components would be required in order to create a macroscopic object.

Performing self-assembly on the macroscale introduces a new set of complications (Whitesides and Boncheva 2002). One fundamentally different aspect is that the assembly elements can be self-propelled as opposed to externally driven as is done on the microscale (Gross and Dorigo 2008). Systems of self-propelled units have been studied in the areas of reconfigurable (Castano et al. 2002) and modular (Dorigo et al. 2004) robotics. The suitability of these systems for programmable matter applications is constrained by the high power requirements for locomotion and limited mobility in three dimensions. Systems with externally propelled components have been used to implement self-replication in one (Penrose and Penrose 1957) and two dimensions (Breivik 2001; Griffith et al. 2005). Self-assembly of predefined shapes has also been demonstrated in two dimensions using passive, non-homogenous, magnetically linking components (Bhalla and Bentley 2006). Systems of homogenous and active components have been used to demonstrate programmable assembly of regular shapes (Klavins 2007) and self-reconfiguration (White et al. 2004) using 12- and 6-cm scale components, respectively. These systems employed an air table to agitate the components; hence they are limited only to 2D structures. Currently there have been only limited attempts to create systems that operate in three dimensions. One successful approach is though self-disassembly (Gilpin et al. 2008). In such a system the components start out in a 3D lattice and detach from each other to form the desired shape. While this simplifies the formation of an initial structure, for it to reconfigure into a general new structure, an assembly technique would be required to reform the original lattice. Another approach is to have the components agitated by a fluid in a 3D chamber as was demonstrated by White et al. (2005). The 10-cm scale of these components, though good for integrating functionality into the components, does not closely approach the resolution necessary for a programmable matter system.

In this work we investigate the use of cm-scale building blocks that are agitated in a stochastic flow pattern and assemble them in using local fluid forces using the general

assembly scheme shown in Fig. 1. Briefly, an assembly substrate provides the pumping force necessary for fluid agitation. As the fluid flows into an open valve on the substrate or building block, a fluidic sink is created. The flow of fluid into this sink will drag free floating blocks towards the associated docking site and align them. This alignment can be facilitated by a secondary force interaction between the docking site and the block; this interaction could be capillary (Gracias et al. 2000), magnetic (Klavins 2007), or geometric (Penrose and Penrose 1957). We have previously analyzed the high-level dynamics of assembly in this type of system using a custom simulator with simplified fluidic forces (Tolley et al. 2010).

In this paper, the crucial problem of component alignment during fluidic assembly is investigated using a combination of numerical simulations and experiments. Numerical simulations were conducted in order to study how blocks approach a sink in a stagnant flow to gain insight into dealing with the degrees of freedom in the system. The numerical results were used to design blocks for experiments in a prototype assembly chamber. These experiments also allowed us to develop strategies for alignment.

2 Theoretical analysis of block assembly

Two sets of simulations were conducted to study 3D hydrodynamically driven assembly. To begin a set of simulations were performed in order to generate a baseline for the motion of an unbiased block toward a fluid sink. The second set of simulations was conducted to test our hypothesis that if the degrees of freedom in the system could be limited alignment would be improved. One rotational degree of freedom could be eliminated by having blocks that align themselves with the gravity field due to an unbalanced mass distribution. Prior to discussing the results of these simulations, in this section details of the numerical method are provided.

In our simulation, the flow was assumed to be laminar and incompressible. The blocks were assumed to be neutrally buoyant and had no initial momentum. The motion of the fluid was described using the 3D, incompressible Navier–Stokes equations for a Newtonian fluid:

$$\frac{\partial u}{\partial t} + u \cdot \nabla u = -\frac{1}{\rho} \nabla p + \nu \nabla^2 u \quad (1)$$

$$\nabla \cdot u = 0 \quad (2)$$

where u is the velocity of the fluid, p is the pressure, and ρ and ν are the density and viscosity of the fluid, respectively. The force, F and torque, T_B on the block are computed using the stress tensor, τ , such that:

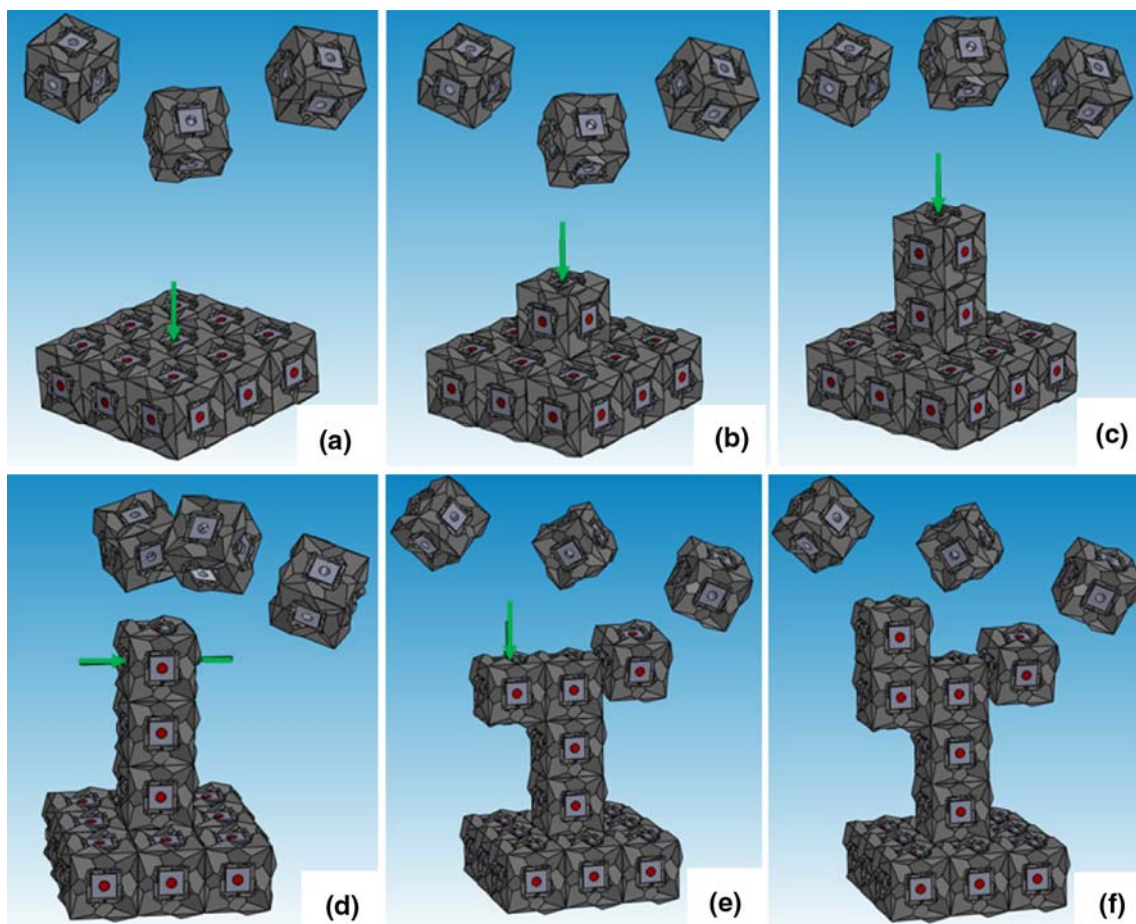


Fig. 1 3D fluidic assembly. **a** Fluid forces attract blocks to the open sink. **b–d** Valves allow for the hydrodynamic affinity of blocks to be controlled to build the desired shape, (*dark* indicates closed, *arrow* indicates open). **e–f** A block that assembles in a misaligned fashion

will not allow assembly to continue. Half of a wrench structure is completed, but assembly of the other half is stopped. A misaligned block can be rejected and assembly could be continued

$$F = \int_A (\tau \cdot n) dA \tag{3}$$

$$T_B = \int_A (r \times (\tau \cdot n)) dA \tag{4}$$

where A is the surface of the body, and n is the surface normal. T_B refers to the torque with respect to the body coordinates. The simulations were performed using the CFD simulation package, FLOW-3D. An explicit method was used to conduct the simulations: fluid and block motions at each time step were calculated using the force and velocity data from the previous time step; similar to the approach taken by Krishnan et al. (2008).

2.1 Characterization of block motion toward docking site as a function of initial conditions

The first set of simulations was conducted to determine the range of initial approach conditions that lead to proper

alignment of blocks at a docking site. The domain was constructed as shown in Fig. 2a. The initial position of the block was varied by setting two angles: The initial polar angle θ between the block and a normal to the sink, and the block’s initial clockwise angle of rotation φ . This setup represents an attempt to model the fact that blocks can approach the sink from any angle and have any orientation with respect to their center of mass. The blocks were started 2 cm away from the sink and were 1 cm on each side. In total 16 simulations were performed, testing the combinations of four values of θ ($0^\circ, 30^\circ, 60^\circ, 90^\circ$) and 4 values of φ ($0^\circ, 15^\circ, 30^\circ, 45^\circ$). The results are shown in Table 1. As expected, the case of $\theta = 0^\circ, \varphi = 0^\circ$ lined up perfectly with the docking site (Fig. 2b). By contrast, the cases of $\theta = 90^\circ$ did not closely approach the docking site since the sink force is weakest parallel to the docking site (the center of the block was more than 6 mm away from the sink, Fig. 2c). In the rest of the cases the block approached the docking site with the corner at an angle, due to the action of hydrodynamic torque (Fig. 2d). This

Fig. 2 Characterization of block motion. **a** The approach angle, θ , and the angular position of the block with respect to its center of mass, ϕ , were varied to over 16 simulation cases. The center-to-center distance between the cube and the sink is a constant 2 cm. **b, c, d** Illustration of the results three example simulation cases, the initial and final position of the block is shown

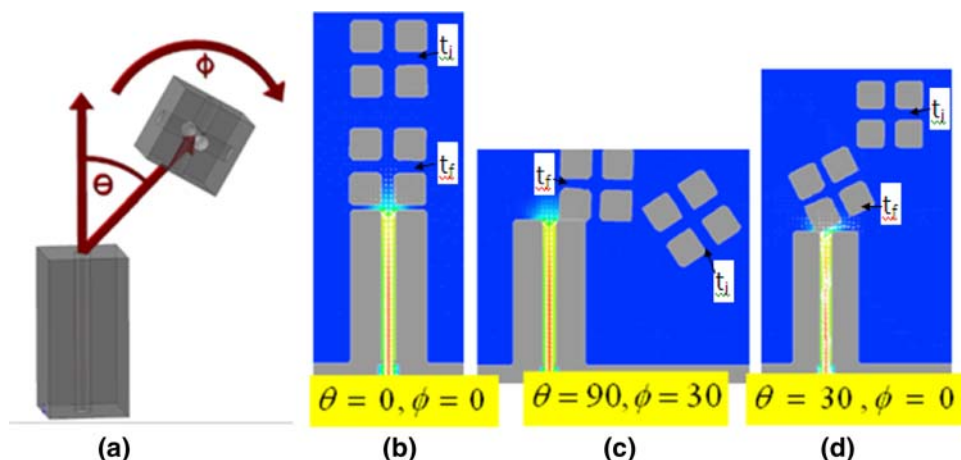


Table 1 Results for uniform block simulations

θ	$\phi = 0^\circ$	$\phi = 15^\circ$	$\phi = 30^\circ$	$\phi = 45^\circ$
0°	Aligned	Corner on	Corner on	Corner on
30°	Corner on	Corner on	Corner on	Corner on
60°	Corner on	Corner on	Corner on	Corner on
90°	6 mm+	6 mm+	6 mm+	6 mm+

type of approach makes it very difficult for any secondary interaction (e.g., magnetic, geometric, or capillary) to align the blocks, since the block is misaligned in all three planes.

2.2 Effect of limiting the degrees of freedom on block alignment

Limiting the degrees of freedom in the motion of the blocks is one method by which the *Corner On* docking observed above could be reduced. This can be done by giving the block an unbalanced mass distribution such that when it is perturbed it experiences a restoring torque to align itself with the gravity field. As a first-order approximation, in our simulations we modeled this by constraining the motion of the moving block so that it could not rotate about the ϕ axis. This assumption is valid so long as restoring torque is much larger than the hydrodynamic torque. The motion of these blocks was simulated for the representative cases shown in Fig. 3 (Tolley et al. 2010). These four cases are: a block was attracted to a wall with a sink, a pedestal with a sink open at the top, a pedestal with a sink open at the side, and a corner structure with two sinks open. In each case, the initial polar angle θ was varied over a range of values and the blocks were initialized 2 cm away from the sink as in the uniform block simulations.

Since these blocks were not allowed to rotate to point an edge at the sink, they could approach the sink and still be in a position to dock. To characterize how well a block docked we use the horizontal component of the final

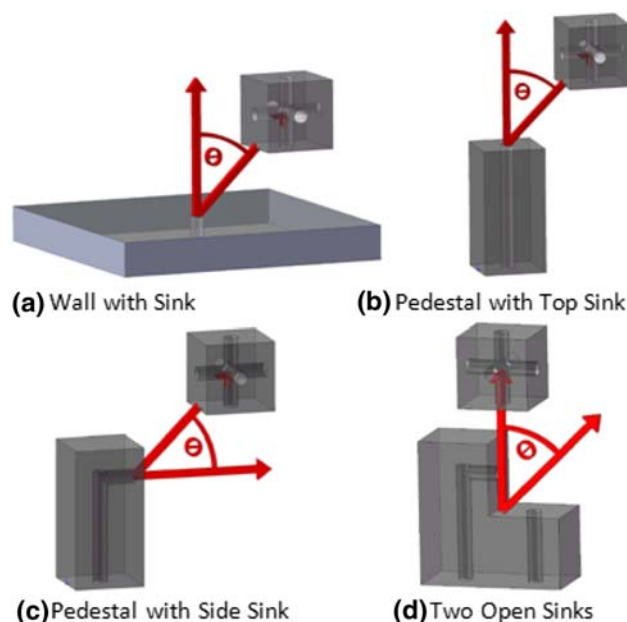
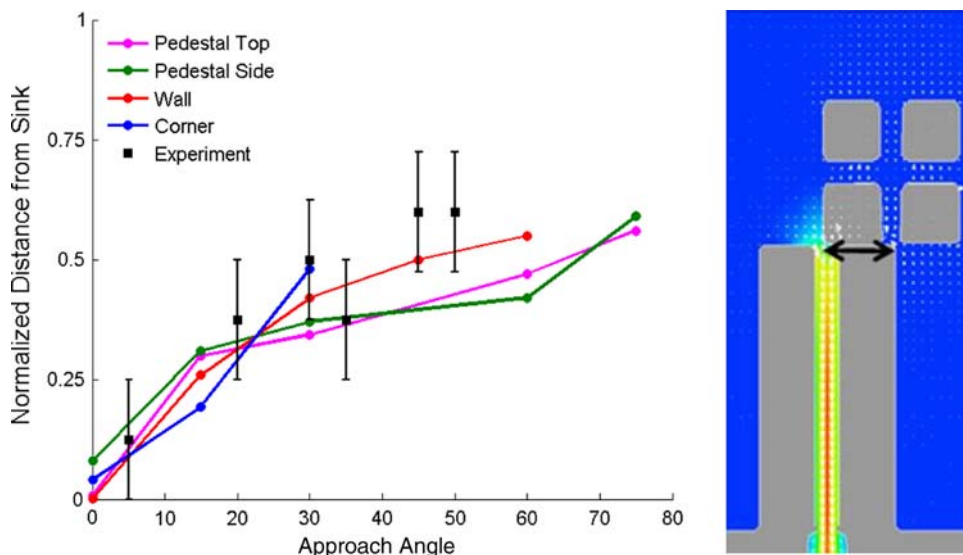


Fig. 3 Basic assembly cases with the variable θ indicated. These four cases represent the possible docking scenarios during the assembly of a large structure (Tolley et al. 2010)

center-to-center distance between the block and the sink, x . This is plotted for the four cases in Fig. 4 for the cases described above. The trends observed for each case are similar, even though the geometry is different. More specifically as θ increases, the block's final position is farther away from the sink increases as well. For the majority of the cases the block comes within 5 mm (50% if normalized by block size) of sink, meaning that it is halfway aligned. The trend is that for each case there is a $\pm 20^\circ$ range in θ that yields a fairly high probability of docking. Beyond this 20° cone performance is poor.

To conclude, the simulations have demonstrated that: (a) the hydrodynamic torque on uniform density blocks will bring them to the docking site in a misaligned corner first

Fig. 4 Simulation results and experimental validation. The final distance (measured as illustrated in the *inset*) between the center of block and sink as a function of the approach angle, θ



position; (b) reducing the rotational degrees of freedom can improve alignment; (c) only a relatively small percentage of blocks will approach close enough to the docking site to allow a secondary interaction to align the block.

3 Experimental characterization of block docking

We performed three sets of experiments to develop and characterize our docking method. The first set of experiments centered on physically implementing our idea for limiting the degrees of freedom of the blocks by giving them an unbalanced mass distribution. In the second set of experiments, we tested the effect of block topography on assembly alignment. In the third set, we developed a protocol for achieving aligned assembly.

An assembly chamber was constructed to carry out these experiments and can be seen in Fig. 5. In this apparatus, water is pumped into the chamber and is allowed to exit through a series of outlets and through the pedestal (which can be seen in the inset) forming a fluid sink at the desired location for the blocks to be attracted. The pressure in the chamber controls the strength of the sink and is set by the inlet pressure regulator. The blocks are agitated in the chamber by a combination of a circulatory flow, which is created by two small circulation pumps, and jet flows from inlets at the top of the chamber. The jets flows were used to push the blocks down since the blocks are buoyant in water. Additionally, a solenoid valve that can be used to create pulsations in the outflow was used in the third set of experiments.

3.1 Experimental validation of simulations

Operation of the assembly chamber is illustrated in Fig. 6, which shows time lapse images of a single cube docking

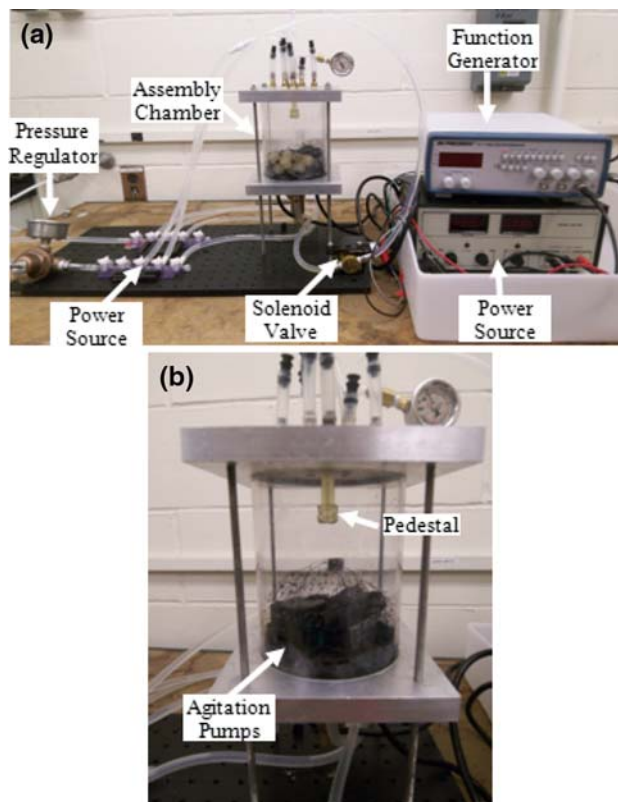
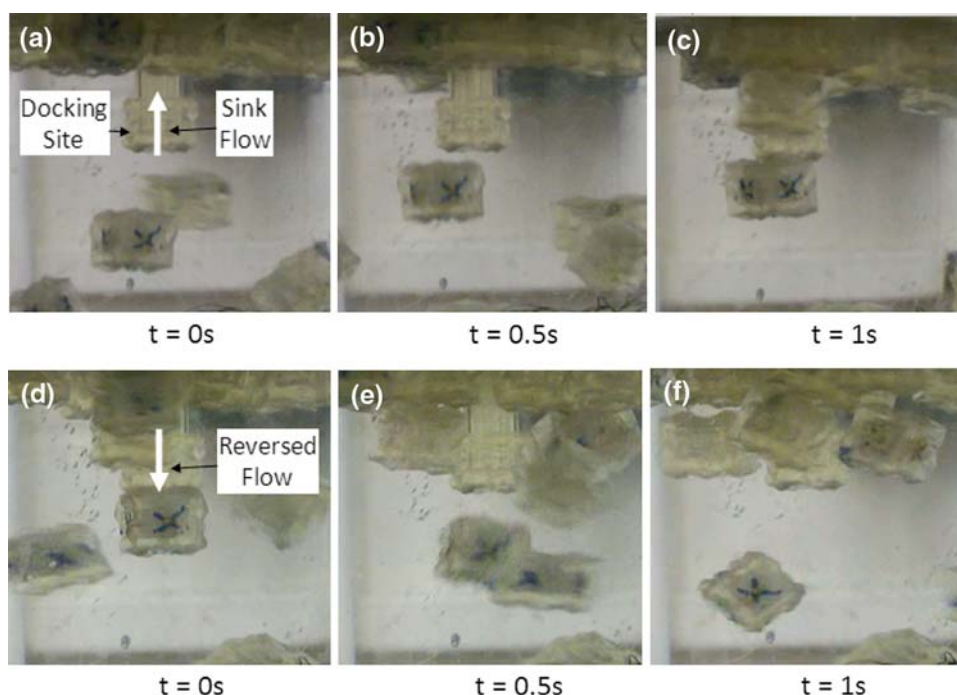


Fig. 5 Assembly chamber for experiments. **a** Overall setup. **b** Close up of chamber. The pressure in the chamber is controlled by an inflow pressure regulator. The assembly chamber has inlets and outlets that are controlled by several valve manifolds. One of the outlets goes through the pedestal docking site. A solenoid valve is used to pulse the flow through the pedestal and is controlled by the function generator and power source (used in the third set of experiments)

and then being rejected from the pedestal. Blocks circulate throughout the chamber and attach to the sink when they approach the sink, as in Fig. 6a–c. Once a block is

Fig. 6 Time lapse images of a block docking and undocking with the pedestal. **a–c** A block from the general flow docks with the pedestal in a misaligned fashion. It is aligned by using the strategy described in Sect. 3.3. **d–f** The block is released from the pedestal by reversing the flow through the sink. This method releases blocks in every case, independent of whether the block aligns or misaligns



attached, it can be aligned (the steps for this are described below in Sect. 3.3), and then rejected to conduct another trial. This cube rejection also demonstrates the system's error correction method and reconfigurability. A video of this operation is presented in Online Resource 1 in Supplementary material.

For successful assembly, blocks have to be aligned to the docking site in three planes. The results of the simulations indicated that alignment in one plane can be generated by making the assembling blocks behave in such a way that one face preferentially orients itself as the top. In these experiments the blocks were manufactured using a 3D printer (rapid prototyping machine) that allowed for a hollow space to be left next to one face of a block, as seen in Fig. 7a. This resulted in the buoyancy-driven restoring torque on the blocks analogous to that described above in the simulations. The blocks used in these experiments were 1 cm on a side. The docking behavior of these blocks was characterized by repeatedly attracting blocks to the pedestal and then releasing them, as in Fig. 6a–c. Their motion was recorded by a camera. 25 blocks were used to populate the chamber in this experiment.

The results of this experiment are presented in Figs. 4a and 7c. In Fig. 4a, the final position of the block with respect to the pedestal is plotted as a function of approach angle for the simulations and the experiment. A similar trend is observed in both cases with smaller angles yielding closer final positions. The experimental results indicate that at high approach angles the final position of the block is worse than predicted by the simulations. This could be due to the fact that the simulations did not

account for the initial translational and rotational momentum of the blocks that is generated by the agitating flow. A histogram of the final positions of the docking block is presented in Fig. 7c. Only in a small percentage of trials (3%), did block ended up in the *Corner On* position: misaligned with its corner in the sink. In 43% of trials the final position of the block was within half the length of the block's side (5 mm). The high percentage of blocks that were outside of this 50% zone is the result of the fact that a majority of the blocks approached the pedestal with high approach angles.

3.2 Effect of block topography

Several block geometries were tested in order to encourage alignment in the two planes perpendicular to the plane of the sink opening. Two representative designs are analyzed here, which we call *Design 1* and *Design 2* (Fig. 8b). When two such blocks were pressed together they self-aligned due to geometric interactions. Additionally, these blocks have latches to stay attached once they are assembled and they are slightly larger than the plain cubes from the previous experiments, 1.2 cm for *Design 1* and 1.5 cm for *Design 2*, due to the limitations of the 3D printer in resolving the added features. We repeated the experiment described in the previous section with these new blocks designs. In these cases, 15–20 blocks were used to populate the chamber and were repeatedly attracted to and released to the pedestal. Adding more blocks would create jamming between them and slow the rate at which trials could be conducted.

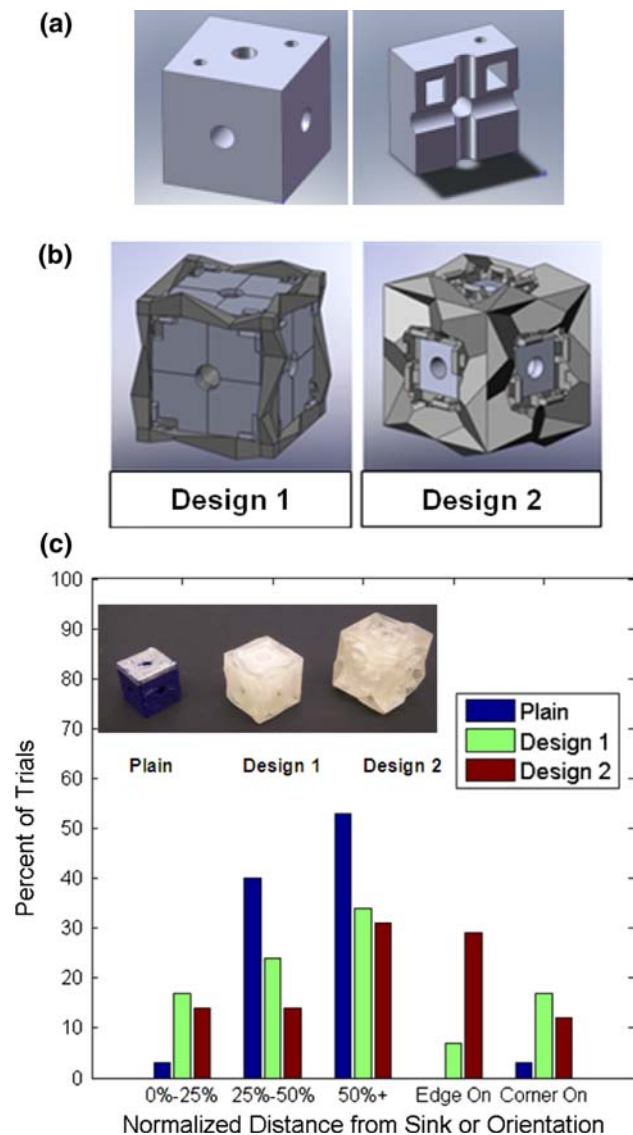


Fig. 7 Effect of block topography. **a** CAD model of 3D-printed cubes with hollow space for an unbalanced mass distribution. **b** CAD models of two block designs that were tested. **c** Histograms of final positions of blocks in for trials with the three block designs shown

The distributions of the final positions of the blocks in each of the experiments are presented in Fig. 8c. The number of blocks that ended very close to the sink (within 25% of the block length) increased for the new designs. An increase in size and weight contributed to this fact since now more blocks approached the pedestal from below and with correspondingly shallower approach angles. Another result is that adding topography to the cube surfaces allowed them to end up in a new final position, which was designated *Edge On*, due to the extra geometric interactions between the block and pedestal surfaces. In this position one edge of the block covers the sink hole in the pedestal, as opposed to *Corner On* where one of the corners covers the

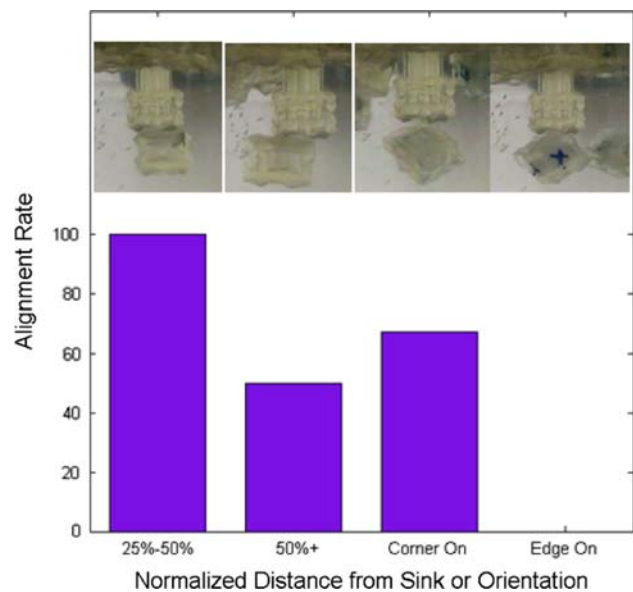


Fig. 8 Initial position of blocks versus alignment. Pulsing the sink flow caused the alignment of majority of blocks whose initial position was not close to the sink or that were in a misaligned orientation in all three planes (corner sucked into sink). In some trials, blocks had their edge sucked into sink and could not be aligned

sink hole. As the geometrical complexity on the block design increased, so did the percentage of trials that reached the *Edge On* position. Though these new block designs also had an unbalanced mass distribution, an increase in the instances of the *Corner On* position was observed, but was kept to below 20%. Most importantly, adding topography to the blocks did not generate aligned assembly.

3.3 Effect of flow pulsation

The experiments described in Sect. 3.2 showed that adding geometric interaction is not enough to generate aligned assembly. A more successful strategy was achieved by adding a solenoid valve to the outflow from the pedestal. This allowed for the flow to be pulsed after a block initially docks in a misaligned manner. The best results were yielded by a 3 Hz pulsation rate, since at this frequency enough block motion was generated to allow the geometric interactions to align the block. At lower frequencies the block could be released to the outer flow, and at higher frequencies the amplitude of the blocks oscillation was too low to allow it to change positions. Experiments were conducted with *Design 1* and *Design 2* blocks. In experiments with the *Design 1*, alignment was never observed over the course of more than 50 trials. However, the *Design 2* blocks were more successful.

During experimental trials with the *Design 2* blocks and flow pulsation, a 54% rate of aligned docking was observed. The average time for a block to get attracted to

the docking site was 30 s, and the average additional time required for a successful alignment was 24 s. The success with which the flow pulsation was able to align the block depended on the initial (misaligned) position that a block took relative to the pedestal (Fig. 8). We observed that the closer the blocks came to the sink initially, the more likely they were to fully align (as expected). Surprisingly, more than half the blocks that misaligned in the *Corner On* position were righted and fully aligned. However, there were trials where blocks reached a position from which it was impossible to achieve alignment (i.e., the previously discussed *Edge On* position).

4 Discussion and conclusions

3D fluidic assembly is an approach that can be used to implement a programmable matter system. In this work we concentrated on understanding the phenomenon at one docking site and demonstrated the ability to assemble a single free floating block using a 3D flow field. Achieving proper alignment is necessary for adding further blocks to the structure and creating larger useful structures. Numerical simulations showed that this cannot be done using fluid motion alone. It was shown that the sink flow can be used to bring blocks to the docking site, but the blocks could be misaligned in all three planes. Blocks with an unbalanced mass distribution were shown to counteract misalignment in the vertical plane. Misalignment in the other two planes was dealt with using two effects. First, blocks were designed to interact with each other through complex geometric interactions. Secondly, a pulsating sink flow facilitated final alignment after a block had been attracted to a docking site. The combination of these methods allowed for the blocks to be successfully docked in 54% of trials. Our system has demonstrated the ability of 3D fluidic assembly to operate on the cm-scale. This is useful for the assembly of macroscale objects with a reasonable resolution. The next steps will be to demonstrate the assembly, reconfiguration, and disassembly of multi-block structures by valving the channels in the blocks.

Acknowledgments We thank Mekala Krishnan, Jonas Neubert, and Abraham Cantwell for useful discussions regarding fluidic assembly and cube design. This work is supported by the Defense Advanced Research Projects Agency Defense Sciences Office under the “Programmable Matter” program.

References

- Avital A, Zussman E (2006) Fluidic assembly of optical components. *IEEE Trans Adv Packag* 29(4):719–724
- Bhalla N, Bentley PJ (2006) Working towards self-assembling robots at all scales. In: Proceedings of the 3rd international conference on autonomous robots and agents, Palmerson North, New Zealand
- Breivik J (2001) Self-organization of template-replicating polymers and the spontaneous rise of genetic informations. *Entropy* 3(4):273–299
- Castano A, Behar A, Will PM (2002) The Conro modules for reconfigurable robots. *IEEE-ASME Trans Mechatronic* 7(4):403–409
- Chung JH, Zheng W, Hatch TJ, Jacobs HO (2006) Programmable reconfigurable self-assembly: parallel heterogeneous integration of chip-scale components on planar and nonplanar surfaces. *J Microelectromech Syst* 15(3):457–464
- Chung SE, Park W, Shin S, Lee SA, Kwon S (2008) Guided and fluidic self-assembly of microstructures using railed microfluidic channels. *Nat Mater* 7(7):581–587
- Dorigo M, Trianni V, Sahin E, Gross R, Labella TH, Baldassarre G, Nolfi S, Deneubourg JL, Mondada F, Floreano D, Gambardella LM (2004) Evolving self-organizing behaviors for a swarm-bot. *Auton Robot* 17(2–3):223–245
- Gilpin K, Kotay K, Rus D, Vasilescu I (2008) Mische: modular shape formation by self-disassembly. *Int J Robot Res* 27(3–4):345–372
- Gracias DH, Tien J, Breen TL, Hsu C, Whitesides GM (2000) Forming electrical networks in three dimensions by self-assembly. *Science* 289(5482):1170–1172
- Griffith S, Goldwater D, Jacobson JM (2005) Robotics—self-replication from random parts. *Nature* 437(7059):636
- Gross R, Dorigo M (2008) Self-assembly at the macroscopic scale. *Proc IEEE* 96(9):1490–1508
- Klavins E (2007) Programmable self-assembly. *IEEE Control Syst Mag* 27(4):43–56
- Krishnan M, Tolley MT, Lipson H, Erickson D (2008) Increased robustness for fluidic self-assembly. *Phys Fluids* 20:1–16
- Liddle JA, Cui Y, Alivisatos P (2004) Lithographically directed self-assembly of nanostructures. *J Vac Sci Technol B* 22(6):3409–3414
- Mastrangeli M, Abbasi S, Varel C, Van Hoof C, Celis JP, Bohringer KF (2009) Self-assembly from milli-to nanoscales: methods and applications. *J Micromech Microeng* 19:1–37
- Morris CJ, Parviz BA (2006) Self-assembly and characterization of Marangoni microfluidic actuators. *J Micromech Microeng* 16(5):972–980
- Penrose LS, Penrose R (1957) Self-reproducing analogue. *Nature* 179(4571):1183
- Sharma R (2007) Thermally controlled fluidic self-assembly. *Langmuir* 23(12):6843–6849
- Srinivasan U, Liepmann D, Howe RT (2001) Microstructure to substrate self-assembly using capillary forces. *J Microelectromech Syst* 10(1):17–24
- Tolley MT, Krishnan M, Erickson D, Lipson H (2008) Dynamically programmable fluidic assembly. *Appl Phys Lett* 93:1–3
- Tolley MT, Kalontarov M, Neubert J, Erickson D, Lipson H (2010) Stochastic modular robotic systems: a study of fluidic assembly strategies. *IEEE Trans Robot* (in press)
- White PJ, Kopanski K, Lipson H (2004) Stochastic self-reconfigurable cellular robotics. In: Proceedings of the 2004 IEEE international conference on robotics and automation, Los Alamitos, CA. Accessed at <http://ccsl.mae.cornell.edu/publications>
- White P, Zykov V, Bongard J, Lipson H (2005) Three dimensional stochastic reconfiguration of modular robots. In: Proceedings of robotics science and systems, MIT Press, Cambridge, MA
- Whitesides GM, Boncheva M (2002) Beyond molecules: self-assembly of mesoscopic and macroscopic components. *Proc Natl Acad Sci USA* 99(8):4769–4774